Non-Dissipative Saturation of the Magneto-Rotational Instability

M. Mond[1], E. Liverts[1], Y. Shtemler[1]
O.M. Umurhan[2], D. Bisikalo[3]

[1]Ben-Gurion University, Israel

[2]University of California Merced, USA

[3]Institute of Astronomy of the Russian Academy of Science, Moscow

Outline

Accretion Disks

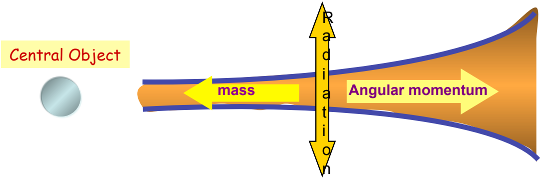

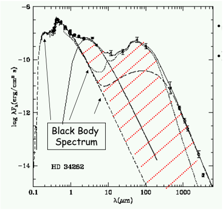

- Turbulence needed to account for angular momentum transfer outwards and excess in infra red radiation.
- What is the source of turbulence in accretion disks ?

Accretion Disks

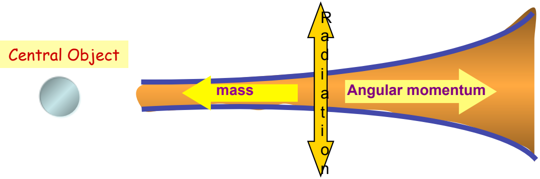

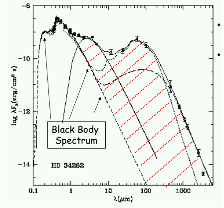

- Turbulence needed to account for angular momentum transfer outwards and excess in infra red radiation.
- What is the source of turbulence in accretion disks ?

Accretion Disks

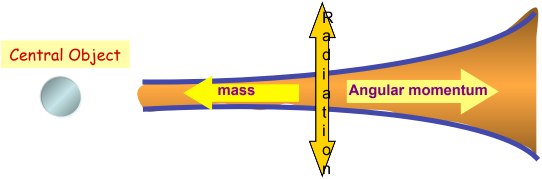

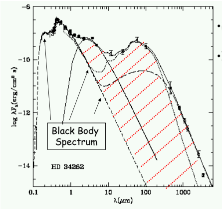

- Turbulence needed to account for angular momentum transfer outwards and excess in infra red radiation.
- What is the source of turbulence in accretion disks ?

The Magnetorotational Instability (MRI)

MRI Wave Pattern

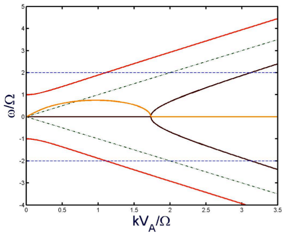

- Balbus & Hawley, 1991.
- Keplerian rotation.
- Infinite cylinder.
- Axisymmetric perturbations.

——— (red)	*Alfvén-Coriolis waves*	.... (green)	*Alfvén waves (no rotation)*
——— (orange)	*MRI*	.... (blue)	*Coriolis (epicyclic) oscillations*

Dissipative Saturation

- Magnetorotational Instability (MRI) [Velikhov (1959), Chandrasekhar (1960)]. Reintroduced by Balbus and Hawley (1991) as a major source of turbulence in thin astrophysical disks.
- Knobloch and Julien (2005) demonstrated saturation of the MRI far from threshold in infinite axially uniform cylindrical plasmas with rigid walls.
- Umurhan et al. (2007) employed the shearing box description in order to show that near threshold the MRI saturation level decreases with the magnetic Prandtl number.
  $A_s \to \sqrt{P_m}, \quad P_m \to 0 : \quad \dot{L} \to 1/Re, \quad Re \to \infty$
- We consider a new dynamical process: non-dissipative saturation in axially stratified thin disks.

Dissipative Saturation

- Magnetorotational Instability (MRI) [Velikhov (1959), Chandrasekhar (1960)]. Reintroduced by Balbus and Hawley (1991) as a major source of turbulence in thin astrophysical disks.
- Knobloch and Julien (2005) demonstrated saturation of the MRI far from threshold in infinite axially uniform cylindrical plasmas with rigid walls.
- Umurhan et al. (2007) employed the shearing box description in order to show that near threshold the MRI saturation level decreases with the magnetic Prandtl number.
  $A_s \to \sqrt{P_m}, \quad P_m \to 0: \quad \dot{L} \to 1/Re, \quad Re \to \infty$
- We consider a new dynamical process: non-dissipative saturation in axially stratified thin disks.

Dissipative Saturation

- Magnetorotational Instability (MRI) [Velikhov (1959), Chandrasekhar (1960)]. Reintroduced by Balbus and Hawley (1991) as a major source of turbulence in thin astrophysical disks.
- Knobloch and Julien (2005) demonstrated saturation of the MRI far from threshold in infinite axially uniform cylindrical plasmas with rigid walls.
- Umurhan et al. (2007) employed the shearing box description in order to show that near threshold the MRI saturation level decreases with the magnetic Prandtl number.
  $A_s \to \sqrt{P_m}, \;\; P_m \to 0 : \;\; \dot{L} \to 1/Re, \;\; Re \to \infty$
- We consider a new dynamical process: non-dissipative saturation in axially stratified thin disks.

Dissipative Saturation

- Magnetorotational Instability (MRI) [Velikhov (1959), Chandrasekhar (1960)]. Reintroduced by Balbus and Hawley (1991) as a major source of turbulence in thin astrophysical disks.
- Knobloch and Julien (2005) demonstrated saturation of the MRI far from threshold in infinite axially uniform cylindrical plasmas with rigid walls.
- Umurhan et al. (2007) employed the shearing box description in order to show that near threshold the MRI saturation level decreases with the magnetic Prandtl number.
  $A_s \to \sqrt{P_m}, \;\; P_m \to 0 : \quad \dot{L} \to 1/Re, \;\; Re \to \infty$
- We consider a new dynamical process: non-dissipative saturation in axially stratified thin disks.

Thin Disk Geometry

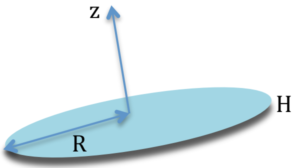

- Axial stretching: $\zeta = \frac{z}{\epsilon}, \quad \epsilon = \frac{H}{R}, \quad \frac{\partial}{\partial z} = \frac{1}{\epsilon}\frac{\partial}{\partial \zeta}.$
- Supersonic rotation: $\textit{Rotation Mach Number} = \frac{1}{\epsilon}.$
- Radial force balance: $v_\theta = r\Omega(r).$
- Axial force balance: $\rho(r,\zeta) = \rho_0(r)e^{-\zeta^2/2H(r)^2}.$
- Free functions: $B_z(r),\ \rho_0(r),\ T(r).$

Thin Disk Geometry

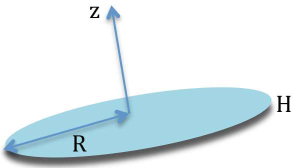

- Axial stretching: $\zeta = \frac{z}{\epsilon}, \quad \epsilon = \frac{H}{R}, \quad \frac{\partial}{\partial z} = \frac{1}{\epsilon}\frac{\partial}{\partial \zeta}.$
- Supersonic rotation: $Rotation\ Mach\ Number = \frac{1}{\epsilon}.$
- Radial force balance: $v_\theta = r\Omega(r).$
- Axial force balance: $\rho(r,\zeta) = \rho_0(r)e^{-\zeta^2/2H(r)^2}.$
- Free functions: $B_z(r),\ \rho_0(r),\ T(r).$

Thin Disk Geometry

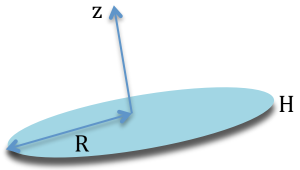

- Axial stretching: $\zeta = \frac{z}{\epsilon}, \quad \epsilon = \frac{H}{R}, \quad \frac{\partial}{\partial z} = \frac{1}{\epsilon}\frac{\partial}{\partial \zeta}.$
- Supersonic rotation: $\textit{Rotation Mach Number} = \frac{1}{\epsilon}.$
- Radial force balance: $v_\theta = r\Omega(r).$
- Axial force balance: $\rho(r,\zeta) = \rho_0(r)e^{-\zeta^2/2H(r)^2}.$
- Free functions: $B_z(r),\ \rho_0(r),\ T(r).$

Thin Disk Geometry

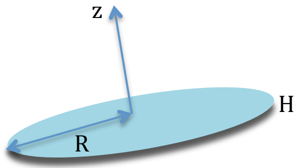

- Axial stretching: $\zeta = \frac{z}{\epsilon}, \quad \epsilon = \frac{H}{R}, \quad \frac{\partial}{\partial z} = \frac{1}{\epsilon}\frac{\partial}{\partial \zeta}.$
- Supersonic rotation: $Rotation\ Mach\ Number = \frac{1}{\epsilon}.$
- Radial force balance: $v_\theta = r\Omega(r).$
- Axial force balance: $\rho(r,\zeta) = \rho_0(r)e^{-\zeta^2/2H(r)^2}.$
- Free functions: $B_z(r),\ \rho_0(r),\ T(r).$

Thin Disk Geometry

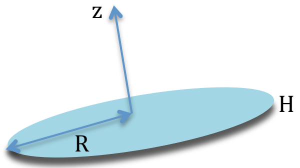

- Axial stretching: $\zeta = \frac{z}{\epsilon}, \quad \epsilon = \frac{H}{R}, \quad \frac{\partial}{\partial z} = \frac{1}{\epsilon}\frac{\partial}{\partial \zeta}.$
- Supersonic rotation: $Rotation\ Mach\ Number = \frac{1}{\epsilon}.$
- Radial force balance: $v_\theta = r\Omega(r).$
- Axial force balance: $\rho(r,\zeta) = \rho_0(r)e^{-\zeta^2/2H(r)^2}.$
- Free functions: $B_z(r),\ \rho_0(r),\ T(r).$

Thin Disk Geometry

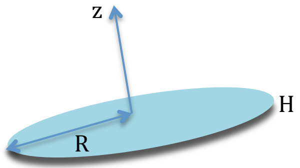

- Axial stretching: $\zeta = \frac{z}{\epsilon}, \quad \epsilon = \frac{H}{R}, \quad \frac{\partial}{\partial z} = \frac{1}{\epsilon}\frac{\partial}{\partial \zeta}.$
- Supersonic rotation: $Rotation\ Mach\ Number = \frac{1}{\epsilon}.$
- Radial force balance: $v_\theta = r\Omega(r).$
- Axial force balance: $\rho(r,\zeta) = \rho_0(r) e^{-\zeta^2/2H(r)^2}.$
- Free functions: $B_z(r),\ \rho_0(r),\ T(r).$

Thin Disk Geometry

Important Parameters

- Plasma beta :

$$\beta(r) = \beta_0 \frac{\rho_0(r)T(r)}{B_z^2(r)}.$$

- Disk semi-thickness:

$$H(r) = \frac{\sqrt{T(r)}}{\Omega(r)}$$

Thin Disk Geometry

Important Parameters

- Plasma beta :

$$\beta(r) = \beta_0 \frac{\rho_0(r)T(r)}{B_z^2(r)}.$$

- Disk semi-thickness:

$$H(r) = \frac{\sqrt{T(r)}}{\Omega(r)}$$

Thin Disk Geometry

Important Parameters

- Plasma beta :

$$\beta(r) = \beta_0 \frac{\rho_0(r)T(r)}{B_z^2(r)}.$$

- Disk semi-thickness:

$$H(r) = \frac{\sqrt{T(r)}}{\Omega(r)}$$

Thin Disk Geometry

Important Parameters

- Plasma beta :

$$\beta(r) = \beta_0 \frac{\rho_0(r) T(r)}{B_z^2(r)}.$$

- Disk semi-thickness:

$$H(r) = \frac{\sqrt{T(r)}}{\Omega(r)}$$

Axial Density Stratification

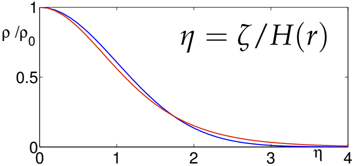

$$\rho/\rho_0 = e^{-\eta^2/2}$$

$$\rho/\rho_0 = sech^2(\eta)$$

The Reduced Thin-Disk MHD Equations

$$\frac{\partial}{\partial t}\begin{bmatrix} x_{ac} \\ x_{ms} \end{bmatrix} = \begin{bmatrix} \mathcal{L}_{ac}(\eta) & 0 \\ 0 & \mathcal{L}_{ms}(\eta) \end{bmatrix}\begin{bmatrix} x_{ac} \\ x_{ms} \end{bmatrix} + \begin{bmatrix} N_{ac}(x_{ac}, x_{ms}) \\ N_{ms}(x_{ac}, x_{ms}) \end{bmatrix}$$

$$x_{ac} \equiv \begin{bmatrix} v_r \\ v_\theta \\ b_r \\ b_\theta \end{bmatrix}$$

Alfven-Coriolis in plane perturbations

$$x_{ms} \equiv \begin{bmatrix} v_z \\ \sigma \end{bmatrix}$$

Magneto-Sonic vertical perturbations

The Reduced Thin-Disk MHD Equations

$$\frac{\partial}{\partial t}\begin{bmatrix} x_{ac} \\ x_{ms} \end{bmatrix} = \begin{bmatrix} \mathcal{L}_{ac}(\eta) & 0 \\ 0 & \mathcal{L}_{ms}(\eta) \end{bmatrix}\begin{bmatrix} x_{ac} \\ x_{ms} \end{bmatrix} + \begin{bmatrix} N_{ac}(x_{ac}, x_{ms}) \\ N_{ms}(x_{ac}, x_{ms}) \end{bmatrix}$$

$$x_{ac} \equiv \begin{bmatrix} v_r \\ v_\theta \\ b_r \\ b_\theta \end{bmatrix}$$

Alfven-Coriolis in plane perturbations

$$x_{ms} = \begin{bmatrix} v_z \\ \sigma \end{bmatrix}$$

Magneto-Sonic vertical perturbations

The Reduced Thin-Disk MHD Equations

$$\frac{\partial}{\partial t}\begin{bmatrix} x_{ac} \\ x_{ms} \end{bmatrix} = \begin{bmatrix} \mathcal{L}_{ac}(\eta) & 0 \\ 0 & \mathcal{L}_{ms}(\eta) \end{bmatrix}\begin{bmatrix} x_{ac} \\ x_{ms} \end{bmatrix} + \begin{bmatrix} N_{ac}(x_{ac}, x_{ms}) \\ N_{ms}(x_{ac}, x_{ms}) \end{bmatrix}$$

$$x_{ac} \equiv \begin{bmatrix} v_r \\ v_\theta \\ b_r \\ b_\theta \end{bmatrix}$$

Alfven-Coriolis in plane perturbations

$$x_{ms} = \begin{bmatrix} v_z \\ \sigma \end{bmatrix}$$

Magneto-Sonic vertical perturbations

The Reduced Thin-Disk MHD Equations

$$\frac{\partial}{\partial t}\begin{bmatrix} x_{ac} \\ x_{ms} \end{bmatrix} = \begin{bmatrix} \mathcal{L}_{ac}(\eta) & 0 \\ 0 & \mathcal{L}_{ms}(\eta) \end{bmatrix}\begin{bmatrix} x_{ac} \\ x_{ms} \end{bmatrix} + \begin{bmatrix} N_{ac}(x_{ac}, x_{ms}) \\ N_{ms}(x_{ac}, x_{ms}) \end{bmatrix}$$

$$x_{ac} \equiv \begin{bmatrix} v_r \\ v_\theta \\ b_r \\ b_\theta \end{bmatrix}$$

Alfven-Coriolis in plane perturbations

$$x_{ms} = \begin{bmatrix} v_z \\ \sigma \end{bmatrix}$$

Magneto-Sonic vertical perturbations

The Reduced Thin-Disk MHD Equations

$$\frac{\partial}{\partial t}\begin{bmatrix} x_{ac} \\ x_{ms} \end{bmatrix} = \begin{bmatrix} \mathcal{L}_{ac}(\eta) & 0 \\ 0 & \mathcal{L}_{ms}(\eta) \end{bmatrix}\begin{bmatrix} x_{ac} \\ x_{ms} \end{bmatrix} + \begin{bmatrix} N_{ac}(x_{ac}, x_{ms}) \\ N_{ms}(x_{ac}, x_{ms}) \end{bmatrix}$$

$$x_{ac} \equiv \begin{bmatrix} v_r \\ v_\theta \\ b_r \\ b_\theta \end{bmatrix}$$

Alfven-Coriolis in plane perturbations

$$x_{ms} = \begin{bmatrix} v_z \\ \sigma \end{bmatrix}$$

Magneto-Sonic vertical perturbations

The Alfvén-Coriolis Spectrum

- Analytical solution for the $\rho/\rho_0 = sech^2(\eta)$ vertical profile.
- Assuming that the perturbations evolve in time as $e^{i\omega\Omega t}$:

$$(L_{ac} + K^+)(L_{ac} + K^-)V_{\theta,r} = 0$$

$$L_{ac} = \frac{d}{d\xi}[(1-\xi^2)\frac{d}{d\xi}], \quad \xi = tanh(\eta), \quad \text{Legendre operator}$$

$$K^{\pm} = \frac{\pi\beta(r)}{4}(3 + 2\omega^2 \pm \sqrt{9 + 16\omega^2})$$

- Solutions diverge at most polynomial at $\eta \to \pm\infty$ if:

$$K^{\pm} = k(k+1)\ , \quad k = 1, 2, \ldots \quad \text{and} \quad v_{\theta,r} = P_k[tanh(\eta)]$$

The Alfvén-Coriolis Spectrum

- Analytical solution for the $\rho/\rho_0 = sech^2(\eta)$ vertical profile.
- Assuming that the perturbations evolve in time as $e^{i\omega\Omega t}$:

$$(L_{ac} + K^+)(L_{ac} + K^-)V_{\theta,r} = 0$$

$$L_{ac} = \frac{d}{d\xi}[(1-\xi^2)\frac{d}{d\xi}], \quad \xi = tanh(\eta),$$ *Legendre operator*

$$K^{\pm} = \frac{\pi\beta(r)}{4}(3 + 2\omega^2 \pm \sqrt{9 + 16\omega^2})$$

- Solutions diverge at most polynomial at $\eta \to \pm\infty$ if:

$$K^{\pm} = k(k+1)\ , \quad k = 1, 2, \ldots \quad \text{and} \quad v_{\theta,r} = P_k[tanh(\eta)]$$

The Alfvén-Coriolis Spectrum

- Analytical solution for the $\rho/\rho_0 = sech^2(\eta)$ vertical profile.
- Assuming that the perturbations evolve in time as $e^{i\omega\Omega t}$:

$$(L_{ac} + K^+)(L_{ac} + K^-)V_{\theta,r} = 0$$

$$L_{ac} = \frac{d}{d\xi}[(1-\xi^2)\frac{d}{d\xi}], \quad \xi = tanh(\eta), \text{ Legendre operator}$$

$$K^{\pm} = \frac{\pi\beta(r)}{4}(3 + 2\omega^2 \pm \sqrt{9 + 16\omega^2})$$

- Solutions diverge at most polynomial at $\eta \to \pm\infty$ if:

$$K^{\pm} = k(k+1)\ , \quad k = 1, 2, \ldots \quad \text{and} \quad v_{\theta,r} = P_k[tanh(\eta)]$$

The Alfvén-Coriolis Eigenfunctions

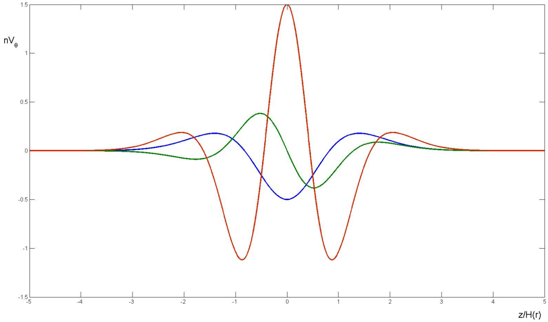

$k = 2$ $k = 3$ $k = 4$

The Alfvén-Coriolis Dispersion Relation - MRI

$$K^{\pm} = k(k+1)$$

$$\Downarrow$$

$$(3\beta_{cr}^{k} - \omega^2\beta)[3\beta_{cr}^{k} - (3+\omega^2)\beta] - 4\omega^2\beta^2 = 0$$

$$\beta_{cr}^{k} \equiv \frac{k(k+1)}{3}$$

k unstable MRI modes for $\beta(r) > \beta_{cr}^{k}$.

The Alfvén-Coriolis Dispersion Relation - MRI

$$K^{\pm} = k(k+1)$$

$$\Downarrow$$

$$(3\beta_{cr}^{k} - \omega^2\beta)[3\beta_{cr}^{k} - (3+\omega^2)\beta] - 4\omega^2\beta^2 = 0$$

$$\beta_{cr}^{k} \equiv \frac{k(k+1)}{3}$$

k unstable MRI modes for $\beta(r) > \beta_{cr}^{k}$.

The Alfvén-Coriolis Dispersion Relation - MRI

$$K^{\pm} = k(k+1)$$

$$\Downarrow$$

$$(3\beta_{cr}^{k} - \omega^2\beta)[3\beta_{cr}^{k} - (3+\omega^2)\beta] - 4\omega^2\beta^2 = 0$$

$$\beta_{cr}^{k} \equiv \frac{k(k+1)}{3}$$

k unstable MRI modes for $\beta(r) > \beta_{cr}^{k}$.

MRI Stability Bifurcation Plot

$$\gamma = Im\omega$$

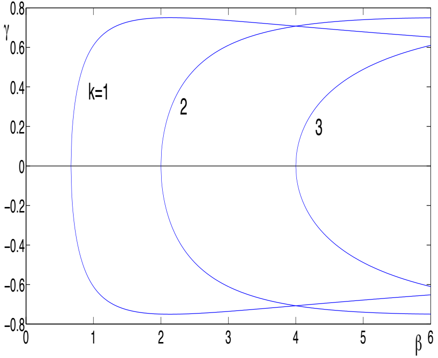

$$\beta^k_{cr} = \frac{k(k+1)}{3}$$

Zero eigenvalue of multiplicity two at each bifurcation point

The Stable Magnetosonic Spectrum

- Analytical solution for the $\rho/\rho_0 = sech^2(\eta)$ vertical profile.
- Assuming that the perturbations evolve in time as $e^{i\omega\Omega t}$:

$$(1-\xi^2)\frac{d^2\sigma}{d\xi^2} + \left[\frac{\omega^2}{1-\xi^2} + 2\right]\sigma = 0, \quad \xi = tanh(\eta)$$

Boundary conditions: $\sigma(\eta) \to 0$ at $\eta \to \pm\infty$ $(\xi \to \pm 1)$

- Usefull substitution:

$$\sigma(\xi) = \sqrt{1-\xi^2} f(\xi)$$

The Stable Magnetosonic Spectrum

- Analytical solution for the $\rho/\rho_0 = sech^2(\eta)$ vertical profile.
- Assuming that the perturbations evolve in time as $e^{i\omega\Omega t}$:

$$(1-\xi^2)\frac{d^2\sigma}{d\xi^2} + \left[\frac{\omega^2}{1-\xi^2} + 2\right]\sigma = 0, \quad \xi = tanh(\eta)$$

Boundary conditions: $\sigma(\eta) \to 0$ at $\eta \to \pm\infty \quad (\xi \to \pm 1)$

- Usefull substitution:

$$\sigma(\xi) = \sqrt{1-\xi^2} f(\xi)$$

The Stable Magnetosonic Spectrum

- Analytical solution for the $\rho/\rho_0 = sech^2(\eta)$ vertical profile.
- Assuming that the perturbations evolve in time as $e^{i\omega\Omega t}$:

$$(1-\xi^2)\frac{d^2\sigma}{d\xi^2} + \left[\frac{\omega^2}{1-\xi^2} + 2\right]\sigma = 0, \quad \xi = tanh(\eta)$$

Boundary conditions: $\sigma(\eta) \to 0$ at $\eta \to \pm\infty$ $\;(\xi \to \pm 1)$

- Usefull substitution:

$$\sigma(\xi) = \sqrt{1-\xi^2} f(\xi)$$

The Stable Magnetosonic Spectrum

- The associated Legendre equations

$$(1-\xi^2)\frac{d^2f}{d\xi^2} - 2\xi\frac{df}{d\xi} + \left[2 - \frac{\mu^2}{1-\xi^2}\right] = 0$$

$$\xi = tanh(\eta), \quad \mu = \sqrt{1-\omega^2}$$

- Solution

$$\sigma(\eta) = \sqrt{1-\xi^2}\,[a_+ f_+(\xi) + a_- f_-(\xi)]$$

$$f_\pm = \left[\frac{1-\xi}{1+\xi}\right]^{\pm\mu/2} (\mu \pm \xi)$$

The Stable Magnetosonic Spectrum

- The associated Legendre equations

$$(1-\xi^2)\frac{d^2f}{d\xi^2} - 2\xi\frac{df}{d\xi} + \left[2 - \frac{\mu^2}{1-\xi^2}\right] = 0$$

$$\xi = tanh(\eta), \quad \mu = \sqrt{1-\omega^2}$$

- Solution

$$\sigma(\eta) = \sqrt{1-\xi^2}\,[a_+f_+(\xi) + a_-f_-(\xi)]$$

$$f_\pm = \left[\frac{1-\xi}{1+\xi}\right]^{\pm\mu/2}(\mu \pm \xi)$$

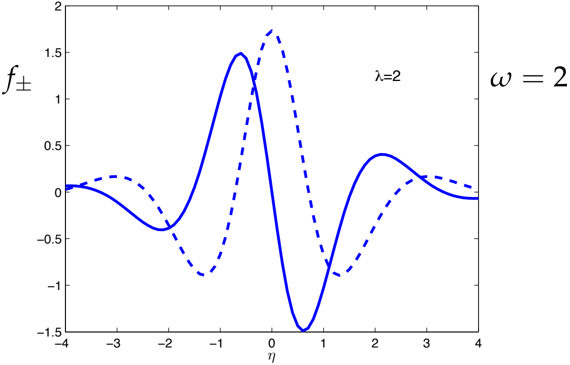

Solutions exist for $\omega^2 > 0$ hence the magnetosonic modes are stable and have a continuous spectrum

Goal

- Consider β values slightly above the threshold of the first unstable mode ($k = 1$): $\beta = \beta^1_{cr} + \delta$
- δ is a control parameter that is related to the growth rate as: $\gamma^2 = 27\delta/14$
- Express any perturbation f as: $f(r, \eta, t) = \phi_1(\eta)a(t)$
- For small perturbations the amplitude is: $a(t) = a_0 e^{\gamma(\delta)t}$.
- Goal of weakly nonlinear analysis: to find differential equation in time for $a(t)$.

Goal

- Consider β values slightly above the threshold of the first unstable mode ($k = 1$): $\beta = \beta_{cr}^{1} + \delta$
- δ is a control parameter that is related to the growth rate as: $\gamma^2 = 27\delta/14$
- Express any perturbation f as: $f(r, \eta, t) = \phi_1(\eta)a(t)$
- For small perturbations the amplitude is: $a(t) = a_0 e^{\gamma(\delta)t}$.
- Goal of weakly nonlinear analysis: to find differential equation in time for $a(t)$.

Goal

- Consider β values slightly above the threshold of the first unstable mode ($k = 1$): $\beta = \beta^1_{cr} + \delta$
- δ is a control parameter that is related to the growth rate as: $\gamma^2 = 27\delta/14$
- Express any perturbation f as: $f(r, \eta, t) = \phi_1(\eta)a(t)$
- For small perturbations the amplitude is: $a(t) = a_0 e^{\gamma(\delta)t}$.
- Goal of weakly nonlinear analysis: to find differential equation in time for $a(t)$.

Goal

- Consider β values slightly above the threshold of the first unstable mode ($k = 1$): $\beta = \beta^1_{cr} + \delta$
- δ is a control parameter that is related to the growth rate as: $\gamma^2 = 27\delta/14$
- Express any perturbation f as: $f(r, \eta, t) = \phi_1(\eta)a(t)$
- For small perturbations the amplitude is: $a(t) = a_0 e^{\gamma(\delta)t}$.
- Goal of weakly nonlinear analysis: to find differential equation in time for $a(t)$.

Goal

- Consider β values slightly above the threshold of the first unstable mode ($k = 1$): $\beta = \beta^1_{cr} + \delta$
- δ is a control parameter that is related to the growth rate as: $\gamma^2 = 27\delta/14$
- Express any perturbation f as: $f(r, \eta, t) = \phi_1(\eta)a(t)$
- For small perturbations the amplitude is: $a(t) = a_0 e^{\gamma(\delta)t}$.
- Goal of weakly nonlinear analysis: to find differential equation in time for $a(t)$.

The Amplitude Equation

- Transition to instability ($\delta = 0$) through double zero eigenvalue.
- Crossing the first instability threshold:
  - The single stable fixed point at the center turns into a (unstable) saddle.
  - Two extra stable fixed points emerge.

The Amplitude Equation

- Transition to instability ($\delta = 0$) through double zero eigenvalue.
- Crossing the first instability threshold:
  - The single stable fixed point at the center turns into a (unstable) saddle.
  - Two extra stable fixed points emerge.

The Amplitude Equation

- Transition to instability ($\delta = 0$) through double zero eigenvalue.
- Crossing the first instability threshold:
    - The single stable fixed point at the center turns into a (unstable) saddle.
    - Two extra stable fixed points emerge.

The Amplitude Equation

- Transition to instability ($\delta = 0$) through double zero eigenvalue.
- Crossing the first instability threshold:
  - The single stable fixed point at the center turns into a (unstable) saddle.
  - Two extra stable fixed points emerge.

The Amplitude Equation

- Transition to instability ($\delta = 0$) through double zero eigenvalue.
- Crossing the first instability threshold:
  - The single stable fixed point at the center turns into a (unstable) saddle.
  - Two extra stable fixed points emerge.

$\delta < 0$

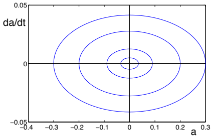

The Amplitude Equation

- Transition to instability ($\delta = 0$) through double zero eigenvalue.
- Crossing the first instability threshold:
  - The single stable fixed point at the center turns into a (unstable) saddle.
  - Two extra stable fixed points emerge.

$\delta < 0$

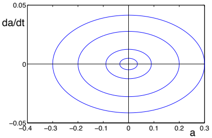

$\delta > 0$

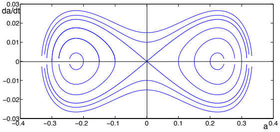

The Amplitude Equation

- Transition to instability ($\delta = 0$) through double zero eigenvalue.
- Crossing the first instability threshold:
    - The single stable fixed point at the center turns into a (unstable) saddle.
    - Two extra stable fixed points emerge.

$\delta < 0$

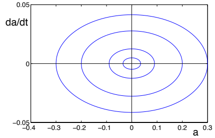

$\delta > 0$

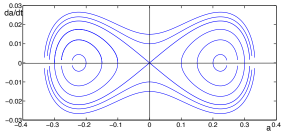

Duffing equation: $\frac{d^2a}{dt^2} = \gamma^2 a - \alpha a^3$

How to Calculate α ?

1. Find the new stable steady-state of the reduced MHD equations:
   - $v_r = v_z = b_\theta = 0, \quad \frac{\partial}{\partial t}(v_\theta, b_r, \sigma) = 0$
   - $b_r(\eta) = \sqrt{\delta}\mu_1\phi_1(\eta) + (\sqrt{\delta})^3\mu_3\phi_3(\eta) + \dots$
2. The equation for ϕ_1 is obtained from lowest order and is:

$$\mathcal{L}(\phi_1) = 0$$

where $\mathcal{L}$ is the linear Alfvén-Coriolis operator.

How to Calculate α ?

1. Find the new stable steady-state of the reduced MHD equations:
   - $v_r = v_z = b_\theta = 0, \quad \frac{\partial}{\partial t}(v_\theta, b_r, \sigma) = 0$
   - $b_r(\eta) = \sqrt{\delta}\mu_1\phi_1(\eta) + (\sqrt{\delta})^3\mu_3\phi_3(\eta) + \ldots$
2. The equation for ϕ_1 is obtained from lowest order and is:

$$\mathcal{L}(\phi_1) = 0$$

where $\mathcal{L}$ is the linear Alfvén-Coriolis operator.

How to Calculate α ?

3. Solution of lowest order linear equation:

$$\phi_1(\eta) = P_0(\xi) - \xi P_1(\xi)$$

4. Next order equation:

$$\mathcal{L}(\phi_3) = \mathcal{N}(\mu_1\phi_1)$$

5. Solvability condition for ϕ_3:

$$< \phi_1\mathcal{N}(\mu_1\phi_1) >= 0$$

Result:

$$\mu_1 = \sqrt{5/2}$$

How to Calculate α ?

3. Solution of lowest order linear equation:

$$\phi_1(\eta) = P_0(\xi) - \xi P_1(\xi)$$

4. Next order equation:

$$\mathcal{L}(\phi_3) = \mathcal{N}(\mu_1 \phi_1)$$

5. Solvability condition for ϕ_3:

$$< \phi_1 \mathcal{N}(\mu_1 \phi_1) >= 0$$

Result:

$$\mu_1 = \sqrt{5/2}$$

How to Calculate α ?

3. Solution of lowest order linear equation:

$$\phi_1(\eta) = P_0(\xi) - \xi P_1(\xi)$$

4. Next order equation:

$$\mathcal{L}(\phi_3) = \mathcal{N}(\mu_1 \phi_1)$$

5. Solvability condition for ϕ_3:

$$< \phi_1 \mathcal{N}(\mu_1 \phi_1) >= 0$$

Result:

$$\mu_1 = \sqrt{5/2}$$

How to Calculate α ?

3. Solution of lowest order linear equation:

$$\phi_1(\eta) = P_0(\xi) - \xi P_1(\xi)$$

4. Next order equation:

$$\mathcal{L}(\phi_3) = \mathcal{N}(\mu_1 \phi_1)$$

5. Solvability condition for ϕ_3:

$$< \phi_1 \mathcal{N}(\mu_1 \phi_1) >= 0$$

Result:

$$\mu_1 = \sqrt{5/2}$$

How to Calculate α ?

6. Back to Duffing's equation ($\ddot{a} = \gamma^2 a - \alpha a^3$)
7. The fixed point is given by:

$$a_0 = \sqrt{\frac{\gamma^2}{\alpha}}$$

8. The fixed point is now identified with the amplitude of the new steady-state of the reduced MHD equations:
9.

$$\alpha = \sqrt{\frac{5}{2}}$$

How to Calculate α ?

6. Back to Duffing's equation ($\ddot{a} = \gamma^2 a - \alpha a^3$)
7. The fixed point is given by:

$$a_0 = \sqrt{\frac{\gamma^2}{\alpha}}$$

8. The fixed point is now identified with the amplitude of the new steady-state of the reduced MHD equations:
9.

$$\alpha = \sqrt{\frac{5}{2}}$$

How to Calculate α ?

6. Back to Duffing's equation ($\ddot{a} = \gamma^2 a - \alpha a^3$)
7. The fixed point is given by:

$$a_0 = \sqrt{\frac{\gamma^2}{\alpha}}$$

8. The fixed point is now identified with the amplitude of the new steady-state of the reduced MHD equations:

9.

$$\alpha = \sqrt{\frac{5}{2}}$$

How to Calculate α ?

6. Back to Duffing's equation ($\ddot{a} = \gamma^2 a - \alpha a^3$)
7. The fixed point is given by:

$$a_0 = \sqrt{\frac{\gamma^2}{\alpha}}$$

8. The fixed point is now identified with the amplitude of the new steady-state of the reduced MHD equations:
9. $$\alpha = \sqrt{\frac{5}{2}}$$

Numerical Calculations

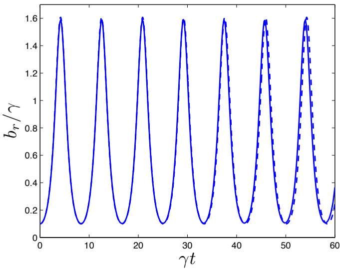

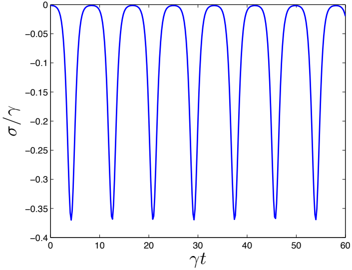

Full line: Duffing Equation

Dashed Line: Nonlinear MHD Equations

The Physical Mechanism

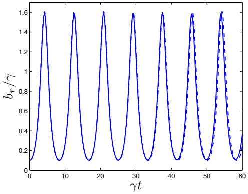

- The growing perturbed magnetic pressure pushes the plasma away and reduces mid-plane density.
- The Alfvén velocity increases.
- The beta value decreases below threshold.

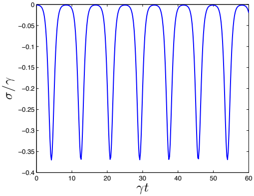

The Physical Mechanism

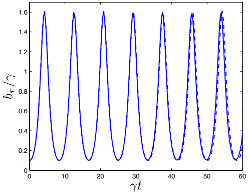

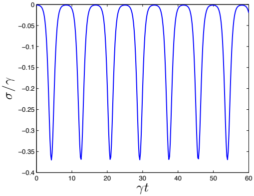

- The growing perturbed magnetic pressure pushes the plasma away and reduces mid-plane density.
- The Alfvén velocity increases.
- The beta value decreases below threshold.

The Physical Mechanism

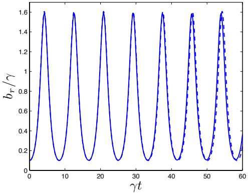

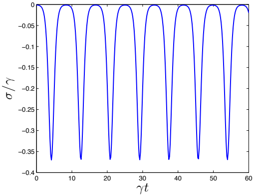

- The growing perturbed magnetic pressure pushes the plasma away and reduces mid-plane density.
- The Alfvén velocity increases.
- The beta value decreases below threshold.

The Physical Mechanism

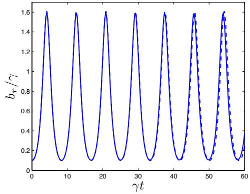

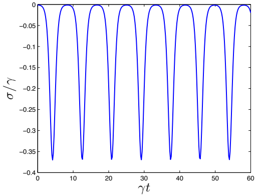

- The growing perturbed magnetic pressure pushes the plasma away and reduces mid-plane density.
- The Alfvén velocity increases.
- The beta value decreases below threshold.

The Physical Mechanism

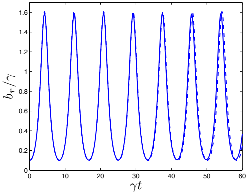

- The growing perturbed magnetic pressure pushes the plasma away and reduces mid-plane density.
- The Alfvén velocity increases.
- The beta value decreases below threshold.

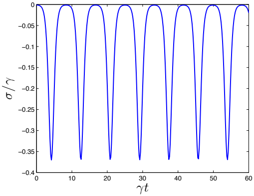

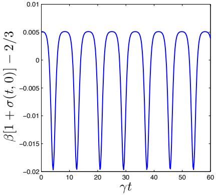

Propertirs of the Weakly Nonlinear Solution

- One conservation law for the amplitude:

$$\left(\frac{da}{dt}\right)^2 + \frac{1}{2}\alpha a^4 - \gamma^2 a^2 = h$$

a(t) is expressed in terms of the Jacobi Elliptic Functions.

$\Rightarrow$ a(t) is bounded.

- Sensitivity of the period of the nonlinear oscillations to Initial Conditions:

$$P \rightarrow \frac{1}{2\gamma} ln\left(\frac{32\gamma^2}{\alpha h}\right) \quad \text{as} \quad h \rightarrow 0$$

Propertirs of the Weakly Nonlinear Solution

- One conservation law for the amplitude:

$$\left(\frac{da}{dt}\right)^2 + \frac{1}{2}\alpha a^4 - \gamma^2 a^2 = h$$

a(t) is expressed in terms of the Jacobi Elliptic Functions.

$\Rightarrow$ a(t) is bounded.

- Sensitivity of the period of the nonlinear oscillations to Initial Conditions:

$$P \to \frac{1}{2\gamma} ln\left(\frac{32\gamma^2}{\alpha h}\right) \quad \text{as} \quad h \to \quad 0$$

Summary

- A new non-dissipative saturation mechanism of the MRI has been demonstrated.
- The MRI excites Magneto-Sonic waves that modify the plasma density.
- The MRI saturates in form of bursty oscillations that drive the system in and out of the stable regime.
- The period of the bursty nonlinear oscillations is sensitive to the initial conditions.

Summary

- A new non-dissipative saturation mechanism of the MRI has been demonstrated.
- The MRI excites Magneto-Sonic waves that modify the plasma density.
- The MRI saturates in form of bursty oscillations that drive the system in and out of the stable regime.
- The period of the bursty nonlinear oscillations is sensitive to the initial conditions.

Summary

- A new non-dissipative saturation mechanism of the MRI has been demonstrated.
- The MRI excites Magneto-Sonic waves that modify the plasma density.
- The MRI saturates in form of bursty oscillations that drive the system in and out of the stable regime.
- The period of the bursty nonlinear oscillations is sensitive to the initial conditions.

Summary

- A new non-dissipative saturation mechanism of the MRI has been demonstrated.
- The MRI excites Magneto-Sonic waves that modify the plasma density.
- The MRI saturates in form of bursty oscillations that drive the system in and out of the stable regime.
- The period of the bursty nonlinear oscillations is sensitive to the initial conditions.

For Further Reading I

- E. Liverts and M. Mond
  MNRAS, 2(1):50–100,
- Y. Shtemler, M. Mond, and E. Liverts
  MNRAS, 2(1):50–100,
- E. Knobloch and K. Julien
  MNRAS, 2(1):50–100,
- O.M. Umurhan, K. Menou, and O.Regev
  MNRAS, 2(1):50–100,
- E. Liverts, Y. Shtemler, M. Mond, O.M. Umurhan, and D. Bisikalo
  Phys. Rev. Lett., 2(1):50–100,

For Further Reading II

O.M. Umurhan and O.Regev.
Fluid Dynamics.
Coming soon to a library near you, 2013.